CrossMark

All-Optical Switching and Routing with a Nonlinear Metamaterial

Xiongshuo Yan[1] · Guanghui Wang[1]

Abstract

We report the dynamic control characteristics of electromagnetic wave propagation in a nonlinear metamaterial by an applied electric field, which is constructed by an array of metallic nanowires embedded into a nonlinear dielectric. Numerical results show that the composite structure can appear three kinds of interesting interconversion characteristics among positive refraction, negative refraction, and cut-off states by adjusting the intensity of the applied electric field. Consequently, we can switch all-optically light states between the total reflection state (OFF state) and the total transmission state (ON state), as well as control light propagation route dynamically. Moreover, we also elaborate on the dependency of the refraction angles of energy flow and wave vector, and Brewster angle on the applied electric field and the orientation angle φ. These properties open up an avenue for potential applications of nonlinear metamaterials in nanophotonic devices such as all-optical switches, routers, and wave cut-off devices.

Introduction

With the rapid progress of modern technology, natural materials are more and more hard to satisfy the requirements of scientific development, and consequently, new kinds of artificially synthetic materials take advantage of the opportunity to exhibit their exotic features and applications [1–6]. At present, many researchers have been turning their attention to metamaterials, which are a kind of artificially composite electromagnetic structures consisting of subwavelength unit cells [7–17]. Artificially engineered metamaterials have shown many unusual electromagnetic properties, for instance, negative refraction [18], ultrahigh-resolution subwavelength imaging [11], self-induced torque [12], spatial filtering, no diffraction transmission [13], and so on. These novel properties are attributed to the fact that they may possess rich dispersion characteristics due to with indefinite permittivity or/and permeability, i.e., not all their tensor components are of the same sign. Owing to the

great progress in fabrication technologies of artificial materials, electromagnetic metamaterials are developed from microwave frequency to terahertz frequency and even to light frequency [1, 5, 19].

It is well known that the earliest proposed metamaterial is an array of thin metallic wires [20–28]. This kind of anisotropic metamaterials (AMMs) have shown that the dielectric constant can be negative in the direction of the metallic wires, as well as many advantages. On the one hand, because the dielectric response in such metamaterials does not require any resonance, the negative refraction for all incident angles has low loss in a broad spectral range, which is a few orders of magnitude lower than that of single-layer metamaterials [18]. Furthermore, this kind of metamaterials can support propagating waves with large wave vectors, while electromagnetic waves are evanescent in usual dielectrics, enabling manipulation of visible light at subwavelength scale. On the other hand, nonlinear metamaterials are also easy to implement, as long as the wire array is embedded into a nonlinear medium with different nonlinear response types [29]. This provides the possibility for us to dynamically manipulate electromagnetic transmission characteristics in nonlinear metamaterials. In many studies of metamaterial systems, their electromagnetic behaviors are based on a local effective medium model, under this condition that the excitations involve a vanishingly small momentum exchange, i.e., a

✉ Guanghui Wang
   wanggh@scnu.edu.cn

[1] Guangdong Provincial Key Laboratory of Nanophotonic
   Functional Materials and Devices, South China Normal
   University, Guangzhou 510006, People's Republic of China

vanishing wave vector [30]. The well-known local response model for the dielectric function of the wire medium is an excellent approximation at high frequencies [31].

At present, controlling electromagnetic characteristics of metamaterials are getting more and more attentions [5, 18]. The applications of metamaterials in all-optical switching and routing have attracted many interests [32–34]. For instance, Shoaei et al. [32] proposed a periodic stack of metal/Al_2O_3/ graphene /Al_2O_3/metal nano-layers metamaterial, where light can be switched between a positive/negative or a negative/no-transmission regime via tuning its chemical potential. But there are still some basic issues to be clarified. For instance, how to control dynamically electromagnetic characteristics of metamaterials? We should also expect dynamic regulation may be achieved by nonlinear effects in metamaterials. In the present paper, we consider the case of nonlinear metamaterials, confirming that it is entirely feasible to dynamically control interconversion between the total reflection state (OFF state) and the total transmission state (ON state), as well as control light propagation route through an external field in such metamaterials. In addition, we demonstrate that these dynamically tunable characteristics have wide applications in all-optical switches, all-optical router, and other nanophotonic devices.

The paper is organized as follows. In section "Basic Theory of Electromagnetic Wave Propagation in AMMs", an anisotropic nonlinear metamaterial is constructed by the periodic array of thin metallic nanowires, and the reflection coefficient and transmission coefficient at the nonlinear metamaterial interface are deduced. In section

"Results and Discussion", the numerical results show that there exist anomalous transmission and reflection in such metamaterial. In particular, these properties can be controlled by an applied electric field and have many potential applications in the field of optoelectronics. Some brief conclusions are presented in section "Conclusions".

Basic Theory of Electromagnetic Wave Propagation in AMMs

In the following, we consider a nonlinear electromagnetic metamaterial, which can be constructed by an array of ideally conducting nanowires embedded into a nonmagnetic host medium with a Kerr-type nonlinearity such as $\varepsilon_h = \epsilon_{D0}(1 + \delta\varepsilon)$ with $\delta\varepsilon = \varkappa \mathbf{e}^* \cdot \mathbf{e}$, where $\mathbf{e}$ is the microscopic electric field and $\varkappa = 3\chi^{(3)}/2\epsilon_{D0}$ is a constant that determines the strength of the nonlinear effects. The geometry of the parallel nanowire array is illustrated in Fig. 1a. It is assumed that the metallic nanowires are cylindrical, and the radius of nanowires and the period of the array are r and a, respectively. Both of them are much smaller than the working wavelength of incident light so that the electromagnetic properties of the component metamaterial can be analyzed by an effective medium theory. As shown schematically in Fig. 1, xoz and $x'oz'$ denote the transmission and principal coordinate systems, respectively. The principal axes of the metamaterial crystal lie along the Cartesian axes x', y', and z'. xz is the plane of incidence, and z is normal to
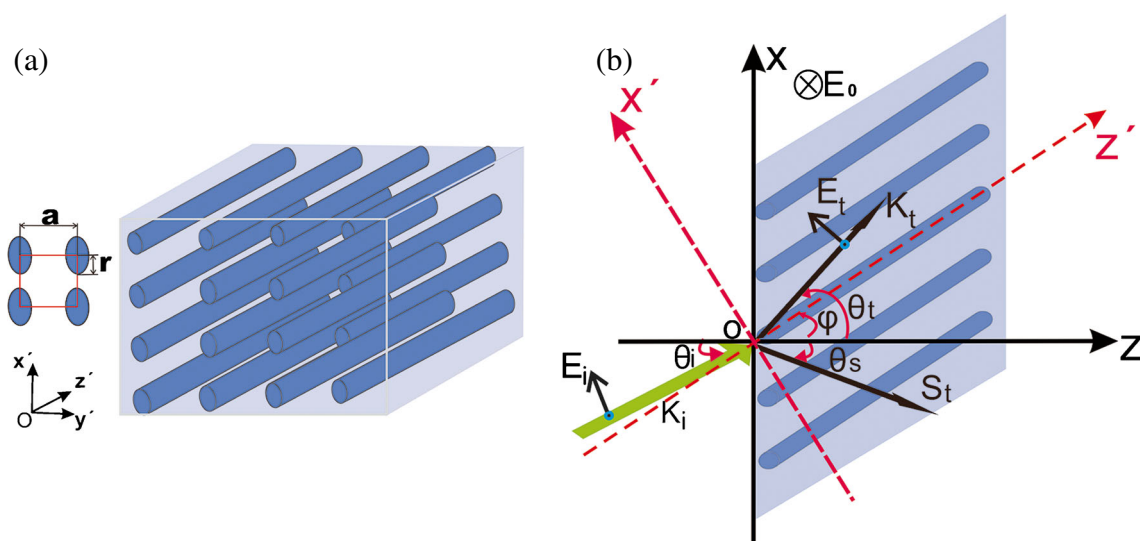
Fig. 1 a Schematic of a nonlinear metamaterial constructed by the periodic array of conducting nanowires embedded into a nonlinear host dielectric. a is the periodic distance between the metallic nanowires; r is the radius of metallic nanowires. **b** Schematic of TM wave in the metamaterial interface. $\mathbf{K}_i$, $\mathbf{K}_t$, and $\mathbf{S}_t$ represent incident wave vector, refraction wave vector, and energy flow vector, respectively; θ_i is the

incident angle; φ is the angle between the transmission coordinate Z axis and principal axis Z', called the orientation angle of the nanowire array; θ_s and θ_t denote the energy-flow and wave-vector refraction angles, respectively. E_0 is an external electric field oriented along the y direction

the slab surface. Without losing generality, we assume that the parallel metallic nanowires are oriented along the z' direction.

In our model, there are two fields, one is the incident field (signal field), and the other is the applied electrostatic field (modulation field). We assume that the incident field (signal field) is a weak field, which only causes the linear response of the medium and does not cause any nonlinear polarization of the medium. However, the applied electrostatic field (modulation field) has a strong intensity. It will cause the third-order nonlinear polarization of the medium with Kerr nonlinearity. In other words, it will cause the nonlinear change of the dielectric constant (or refractive index) of the medium. This refractive index change will modulate the propagation characteristics of the incident field (signal field) with a weak intensity. It is well known that the relative dielectric permittivity tensor $\widehat{\varepsilon}$ of the anisotropic metamaterial has the following diagonalizable form [35, 36]:

$$\widehat{\varepsilon} = \begin{pmatrix} \varepsilon_x & 0 & 0 \\ 0 & \varepsilon_y & 0 \\ 0 & 0 & \varepsilon_z \end{pmatrix} \quad (1)$$

in the principal coordinate system. If an electrostatic field E_0 is applied in the y direction, the elements of the dielectric tensor $\widehat{\varepsilon}$ of the electromagnetic metamaterial, caused by the modulation field E_0, can be expressed as the following forms [7]:

$$\varepsilon_x = \epsilon_D(E_0^2) = \epsilon_{D0} + \zeta E_0^2/E_c^2 \quad (2)$$

$$\varepsilon_y = \epsilon_{D0} + \zeta E_0^2/E_{cy}^2 \quad (3)$$

$$\varepsilon_z = \epsilon_D(E_0^2) - \frac{\omega_p^2}{\omega(\omega - i\gamma_\epsilon)} \quad (4)$$

according to the theory of nonlinear optics and Drude model, where ε_z denotes the effective nonlinear dielectric permittivity of the electromagnetic metamaterial along the direction of the nanowires (namely, the z' direction), and $\omega_p \approx (c/a)[2\pi/\ln(a/r)]^{1/2}$ is the effective plasma frequency, $\gamma_\epsilon = c^2/2\sigma S \ln(a/r)$ (in the case of low losses, $\gamma_\epsilon \ll \omega$), c is the speed of light, σ is the conductivity of the metal wires, and S is the effective area of the wire cross section, respectively [7]. ϵ_{D0} is the linear dielectric constant of the dielectric substrate, E_c and E_{cy} are two characteristic parameters that determine the strength of the nonlinear effects, which are related to the third-order nonlinear susceptibility $\chi^{(3)}$ of the host medium, namely, $1/E_c^2 = 3\left|\chi^{(3)}_{xxyy}\right|/2 = 3\left|\chi^{(3)}_{zzyy}\right|/2$, and $1/E_{cy}^2 = 3\left|\chi^{(3)}_{yyyy}\right|/2$. In addition, $\zeta = \pm 1$ stand for a focusing and defocusing nonlinearity, respectively. For the sake of simplicity, we will not consider losses and spatial dispersion effect of the system in the following.

Based on Eqs. 2 and 4, Fig. 2 shows the dependence of ε_x and ε_z on the normalized intensity of the applied electric field E_0^2/E_c^2, in which (a) and (b) correspond to a focusing and defocusing nonlinearity, respectively. It is not hard to see that there exists different relationship between ε_z (or ε_x) and the external electric field E_0 for different nonlinear response types. It is worth noting that it is accessible to control the value and sign of the effective dielectric permittivity ε_z via changing the normalized intensity of external electric field, E_0^2/E_c^2. In Fig. 2, we can see that with E_0^2/E_c^2 increasing, both ε_x and ε_z increase linearly for a focusing nonlinearity ($\zeta = 1$), while they decrease linearly for a defocusing nonlinearity ($\zeta = -1$). It is important to note that the sign of ε_z can be changed for both focusing and defocusing nonlinearity with the external electric field intensity increasing, providing a feasible way for us to
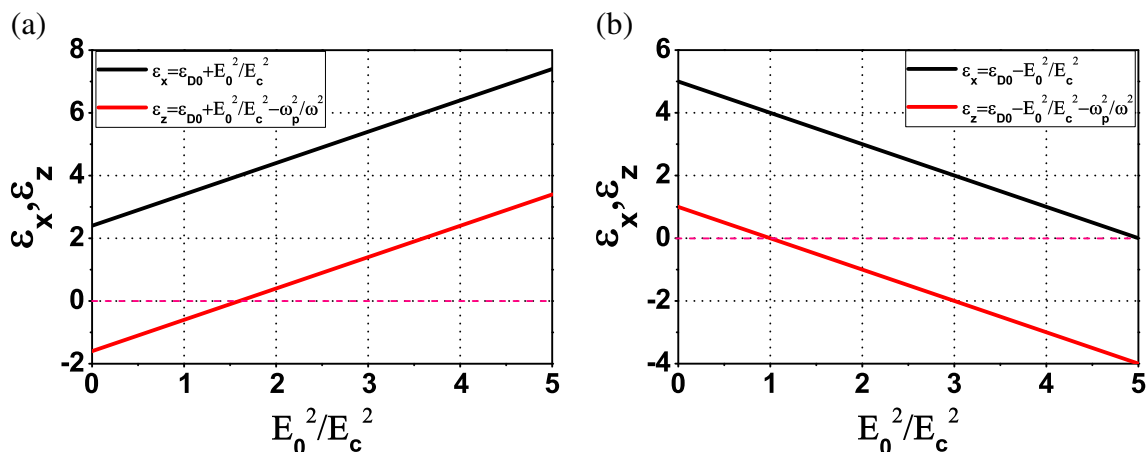
Fig. 2 Effective relative dielectric permittivities ε_x and ε_z versus the normalized intensity of external electric field E_0^2/E_c^2 for two cases: **a** $\zeta = 1$ (for self-focusing nonlinearity), and $\varepsilon_{D0} = 2.4$, **b** $\zeta = -1$ (for self-defocusing nonlinearity), and $\varepsilon_{D0} = 6$

dynamically control the transmission characteristics of electromagnetic wave in the nonlinear metamaterials. The underlying physics is due to the excitation of surface plasmon polariton (SPP) along the direction of the metallic wires in the metamaterials, which makes it is possible that the effective dielectric permittivity ε_z of the metamaterials is negative. But it is worth emphasizing that ε_x should always be positive due to the lack of SPP excitation in the x' direction.

In what follows, we consider that a transverse magnetic (TM) wave propagates from air into the composite metamaterial structure with an incident angle θ and angular frequency ω, as shown in Fig. 1b. The time-harmonic magnetic field polarizing along the y axis has the form

$$\mathbf{H}_i = H_0 \mathbf{e}_y \exp(ik_x x + ik_z z - i\omega t) \tag{5}$$

where H_0 is the amplitude of the incident magnetic field. k_x and k_z are the x- and z-axis components of the incident wave vector in air dielectric, respectively. By transforming the principal coordinate system $(x'oz')$ into transmission coordinate system (xoz) via Euler transformation [37], then the relative dielectric permittivity tensor $\widehat{\varepsilon}$ in the transmission axis coordinate system can be written as

$$
\widehat{\varepsilon} = \begin{pmatrix} \varepsilon_{xx} & 0 & \varepsilon_{xz} \\ 0 & \varepsilon_{yy} & 0 \\ \varepsilon_{zx} & 0 & \varepsilon_{zz} \end{pmatrix}
$$
$$
= \begin{pmatrix} \varepsilon_x \cos^2\varphi + \varepsilon_z \sin^2\varphi & 0 & (\varepsilon_x - \varepsilon_z)\sin\varphi\cos\varphi \\ 0 & \varepsilon_y & 0 \\ (\varepsilon_x - \varepsilon_z)\sin\varphi\cos\varphi & 0 & \varepsilon_z \cos^2\varphi + \varepsilon_x \sin^2\varphi \end{pmatrix} \tag{6}
$$

Based on Eq. 6 and Maxwell's equations, it is not hard to get the dispersion equation in the composite anisotropic metamaterial as follows:

$$\alpha k_{tz}^2 + \beta k_{tx}^2 + \eta k_{tz} k_{tx} = \frac{\omega^2}{c^2} \tag{7}$$

where k_{tx} and k_{tz} are the x and z components of the refraction wave vector, respectively, and

$$\alpha = \frac{1}{\mu_y \varepsilon_x \varepsilon_z} (\varepsilon_x \sin^2\varphi + \varepsilon_z \cos^2\varphi) \tag{8}$$

$$\beta = \frac{1}{\mu_y \varepsilon_x \varepsilon_z} (\varepsilon_x \cos^2\varphi + \varepsilon_z \sin^2\varphi) \tag{9}$$

$$\eta = \frac{1}{\mu_y \varepsilon_x \varepsilon_z} (\varepsilon_x \sin 2\varphi - \varepsilon_z \sin 2\varphi) \tag{10}$$

where φ is the angle between the transmission axis and principal axis, and μ_y is the relative permeability of the metamaterial in the y direction [35]. From the dispersion

Eq. 7, we can derive that the z component of the refraction wave vector has the following form

$$k_{tz} = \frac{-\eta k_{tx} + \delta\sqrt{(\eta^2 - 4\alpha\beta)k_{tx}^2 + 4\alpha\omega^2/c^2}}{2\alpha} \tag{11}$$

where $k_{tx} = k_x$ due to the phase matching condition at the interface; $\delta = \pm 1$ to ensure compliance with the law of energy conservation.

From Eq. 11, we can know that if the incident electromagnetic wave can transmit inside the right-side composite metamaterial structure, as shown in Fig. 1b, it is necessary to satisfy the inequation [35]

$$\varepsilon_r \mu_r (\eta^2 - 4\alpha\beta)\sin\theta + 4\alpha > 0 \tag{12}$$

where ε_r and μ_r are the relative permittivity and permeability of air, respectively. By Fresnel equations, we can deduce the reflection coefficient R and transmission coefficient T at the interface between air and the composite metamaterial structure as follows:

$$R = -1 + \frac{4k_z}{2k_z + \varepsilon_r \mu_y k_{tx}\gamma + 2\varepsilon_r \mu_y \alpha k_{tz}} \tag{13}$$

$$T = \frac{4k_z}{2k_z + \varepsilon_r \mu_y k_{tx}\gamma + 2\varepsilon_r \mu_y \alpha k_{tz}} \tag{14}$$

respectively. Based on the definition of the time averaged Poynting vector $\langle \mathbf{S} \rangle = \frac{1}{2}\mathrm{Re}[\mathbf{E}\times\mathbf{H}^*]$, the averaged Poynting vector of incident wave can be deduced as follows:

$$\langle \mathbf{S_i} \rangle = \frac{1}{2}\mathrm{Re}[\mathbf{E}_i \times \mathbf{H}_i^*]$$
$$= \mathrm{Re}\left[\frac{H_0^2 k_x}{2\varepsilon_0 \varepsilon_r \omega}\mathbf{e}_x + \frac{H_0^2 k_z}{2\varepsilon_0 \varepsilon_r \omega}\mathbf{e}_z \right] \tag{15}$$

and the time averaged Poynting vector of refracted wave is

$$\langle \mathbf{S_t} \rangle = \frac{1}{2}\mathrm{Re}[\mathbf{E}_t \times \mathbf{H}_t^*]$$
$$= \frac{1}{2}\mu_y H_0^2 |T|^2$$
$$\times \mathrm{Re}\left\{ \left[\left(\frac{k_{tx}\beta}{\varepsilon_0\omega} + \frac{k_{tz}\eta}{2\omega\varepsilon_0} \right)\mathbf{e}_x + \left(\frac{k_{tz}\alpha}{\omega\varepsilon_0} + \frac{k_{tx}\eta}{2\omega\varepsilon_0} \right)\mathbf{e}_z \right] \right.$$
$$\left. \times \exp[i(k_{tz} - k_{tz}^*)] \right\} \tag{16}$$

From Eq. 16, we can derive that

$$\mathbf{e}_z \cdot \langle \mathbf{S_t} \rangle = \frac{1}{2}\mathrm{Re}\left[\frac{k_{tx}\varepsilon_{xz} + k_{tz}\varepsilon_{zz}}{\varepsilon_0\omega\varepsilon_x\varepsilon_z} H_0^2 |T|^2 \exp[i(k_{tz} - k_{tz}^*)z] \right] \tag{17}$$

Then in Eq. 11, when $\Delta = (\eta^2 - 4\alpha\beta)k_{tx}^2 + 4\alpha\omega^2/c^2 < 0$

$$k_{tz} = \frac{-\eta k_{tx} + \delta\sqrt{|\Delta|}i}{2\alpha} \tag{18}$$

where $\delta = \pm 1$, and i is the imaginary unit, therefore k_{tz} is a complex number. What's more, from Eqs. 17 and 18, we can obtain

$$\mathbf{e}_z \cdot \langle \mathbf{S_t} \rangle = \mathrm{Re}\left[\frac{\pm \varepsilon_{zz}\sqrt{|\Delta|}i}{4\alpha\varepsilon_0\omega\varepsilon_x\varepsilon_z}H_0^2|T|^2 \exp i(k_{tz}-k_{tz}^*)z\right] = 0$$

This means, for the transmission wave, there is no energy flow along the z-axis. In other words, when the condition $\Delta = (\eta^2 - 4\alpha\beta)k_{tx}^2 + 4\alpha\omega^2/c^2 < 0$ is satisfied, all of incident waves are reflected totally.

What's more, we obtain the transmissivity and energy-flow angle from Eq. 16 as follows:

$$t = \frac{\mu_y\varepsilon_r|T|^2(k_{tx}\eta + 2k_{tz}\alpha)}{2k_z} \tag{19}$$

$$\theta_s = \tan^{-1}\frac{(4\alpha\beta-\eta^2)\sqrt{\varepsilon_r\mu_r}\sin\theta_i + \eta\sqrt{(\eta^2-4\alpha\beta)\varepsilon_r\mu_r\sin^2\theta_i + 4\alpha}}{2\alpha\sqrt{(\eta^2-4\alpha\beta)\varepsilon_r\mu_r\sin^2\theta_i + 4\alpha}} \tag{20}$$

respectively [35]. In addition, based on the definition of wave-vector refraction angle, $\theta_t = \tan^{-1}k_x/k_{tz}$, we can get its specific expression from Eq. 11 as

$$\theta_t = \tan^{-1}\frac{\sqrt{\varepsilon_r\mu_r}2\alpha\sin\theta_i}{-\eta\sqrt{\varepsilon_r\mu_r}\sin\theta_i + \sqrt{(\eta^2-4\alpha\beta)\varepsilon_r\mu_r\sin^2\theta_i + 4\alpha}} \tag{21}$$

Results and Discussion

In what follows, some parameters used in our numerical calculations are adopted as $\varepsilon_r = \mu_r = 1$, $\mu_y = 1$, and incident light frequency $\omega = \omega_p/2$. At first, we need to define the positive and negative value of angle. Generally, it is based on this rule that beginning from the normal line of interface and pointing to incident rays or refracted lines, if it is clockwise, then the angle is negative; otherwise, the angle is positive. And thus, we can determine whether it is a positive or negative refraction for both energy flow and wave vector. When the incident angle and refraction angle is the same sign, the incident ray and the refracted one are located on both sides of the normal line, then it is regarded as positive refraction. If the incident angle and refraction angle has different sign, the incident ray and the refracted one are located at the same side of the normal line, then it is negative refraction [35].

Comparing Eqs. 20 and 21, we can see that the direction of the energy flow and wave vector should be inconsistent with each other in anisotropic metamaterials generally. To see the difference between them, we plot the energy-flow refraction angle θ_s, the wave-vector refraction angle θ_t, and their included angle $|\theta_s - \theta_t|$ as a function of incident angle θ_i for different orientation angle φ of the nanowire array in the absence of nonlinear response for two cases: (1) $\epsilon_{D0} = 2.4$; (2) $\epsilon_{D0} = 6$ in Fig. 3. It is worth emphasizing that when $\epsilon_{D0} = 6.0$, $\varepsilon_x > 0$ and $\varepsilon_z > 0$; when $\epsilon_{D0} = 2.4$, $\varepsilon_x > 0$ and $\varepsilon_z < 0$. The two cases correspond to the dielectric properties in the limit of $E_0^2/E_c^2 = 0$ in Fig. 2b, a, respectively.

Linear Response with $\varepsilon_x > 0$ and $\varepsilon_z > 0$

In Fig. 3a–c with $\epsilon_{D0} = 6$, corresponding to the case of $\varepsilon_x > 0$ and $\varepsilon_z > 0$, we can see that the refraction wave-vector angle θ_t has always the same sign as the incident angle θ_i for any orientation angle φ, as shown in Fig. 3a; therefore, the wave vector is always positive refraction at the metamaterial interface, which is consistent with that in usual anisotropic materials. However, whether the energy flow is positive or negative refraction depends on the orientation angle φ. From Fig. 3b, one can see that when $\varphi = 0°$, the energy-flow angle θ_s has always the same sign as θ_i for any incident angle; therefore, the energy flow is always positive refraction when $\varphi = 0°$. But when $\varphi \neq 0°$, θ_s has the same sign as θ_i except for the cases of $0 < \theta_I < \theta_c(\varphi) = \sin^{-1}\sqrt{\frac{\eta^2}{\varepsilon_r\mu_r\beta(4\alpha\beta - \eta^2)}}$, as shown in the green shaded area in Fig. 3b. Here, it is worthy noting that the critical incident angle θ_c depends on the orientation angle φ. This indicates that if we choose a suitable orientation angle φ, it is also possible that the energy flow is negative refraction in the case of $\varepsilon_x > 0$ and $\varepsilon_z > 0$, and the region of negative refraction is tunable by the orientation angle φ.

Linear Response with $\varepsilon_x > 0$ and $\varepsilon_z < 0$

In Fig. 3d–f with $\epsilon_{D0} = 2.4$, corresponding to the case of $\varepsilon_x > 0$ and $\varepsilon_z < 0$, it is not hard to see some important properties as follows: (1) when $\varphi = 0°$, θ_t has the same sign as θ_i for any incident angle; therefore, the wave vector is always positive refraction. But θ_s has opposite sign with θ_i, therefore, the energy flow is always negative refraction, which is evidently different from the case of $\epsilon_{D0} = 6$ (namely $\varepsilon_x > 0$ and $\varepsilon_z > 0$). In the particular case of $\theta_i = 0°$, i.e., the normal incidence, both θ_s and θ_t are 0, meaning the refraction wave vector is coincident with the Poynting vector, and light travels in straight lines at the metamaterial interface. Therefore, the energy flow belongs to all-angle negative refraction for any incident angle except for $\theta_i = 0°$. The property is absent in usual anisotropic materials. (2) When $\varphi = -30°$, the wave vector is always positive refraction for any incident angle, but the refractive properties of the energy flow depend on the sign of incidence angle. Specifically, when $-90° < \theta_i < 0°$, θ_s has the different sign with θ_i;

Fig. 3 The energy-flow refraction angle θ_s, the wave-vector refraction angle θ_t, and their included angle $|\theta_s - \theta_t|$ versus the incident angle θ_i with different orientation angles φ of the nanowire array in the limit of $E_0^2/E_c^2 = 0$ for two cases: (1) $\epsilon_{D0} = 6$ (the left column (**a, b, c**)); (2) $\epsilon_{D0} = 2.4$ (the right column (**d, e, f**))
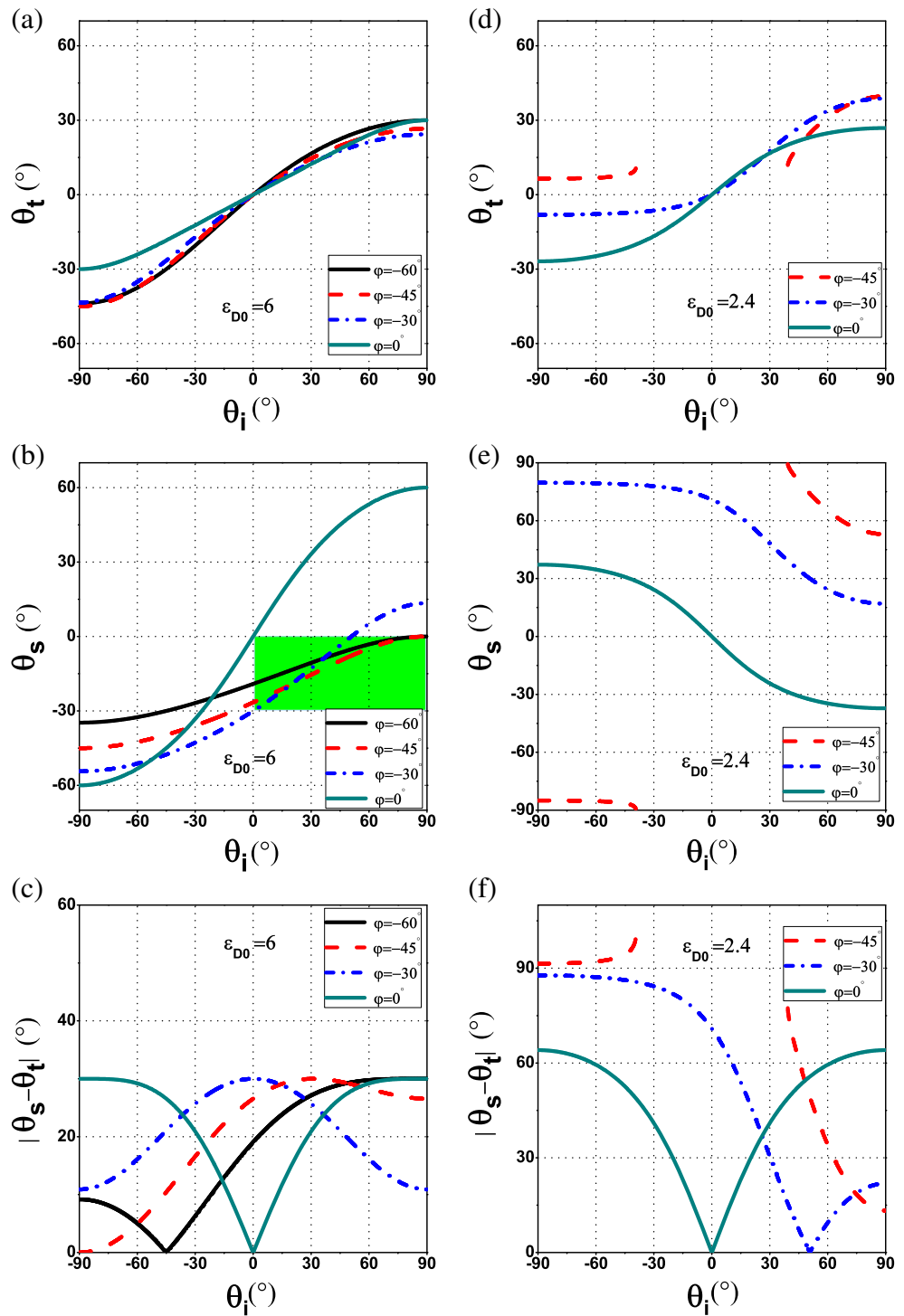
therefore, the energy flow is negative refraction; when $0° < \theta_i < 90°$, the energy-flow angle is positive; consequently, it is positive refraction. (3) For a fixed orientation angle $\varphi = -45°$, we can get when $-\pi/2 < \theta_i < -\sin^{-1}\sqrt{\frac{-4\alpha}{\eta^2 - 4\alpha\beta}}$, $\theta_s < 0$ and the energy-flow refraction would be positive, but $\theta_t > 0$ and the wave vector refraction

is negative; if $\sin^{-1}\sqrt{\frac{-4\alpha}{\eta^2 - 4\alpha\beta}} < \theta_i < \pi/2$, then $\theta_s > 0$ and $\theta_t > 0$; therefore, both the wave vector and energy flow are positive refraction; if $-\sin^{-1}\sqrt{\frac{-4\alpha}{\eta^2 - 4\alpha\beta}} < \theta_i < \sin^{-1}\sqrt{\frac{-4\alpha}{\eta^2 - 4\alpha\beta}}$, there exist not any wave vector and energy-flow refraction angles, meaning no energy can be

transmitted and total reflection phenomena occur. This property is also absent in usual anisotropic materials. Here, $\theta_{c1}(\varphi) = \pm \sin^{-1}\sqrt{\frac{-4\alpha}{\eta^2 - 4\alpha\beta}}$ are two critical angles, and when $\varphi = -45°$, $\theta_{c1} = \pm 39.22°$.

Figure 3c, f shows the included angle between the refraction wave vector $\mathbf{k}_t$ and the average Poynting vector $\langle \mathbf{S}_t \rangle$. We can see that the included angle in anisotropic metamaterials may be much larger than that in usual anisotropic materials. For instance, in the case of $\epsilon_{D0} = 2.4$ in Fig. 3f, when $\varphi = -45°$, the included angle between $\mathbf{k}_t$ and $\langle \mathbf{S}_t \rangle$ is in the region from 90° to 270° for $-90° < \theta_i < -39.22°$, implying a backward wave will occur according to the definition of backward wave. What's more, when $\varphi = 0°$, the included angle between the refraction wave vector and the Poynting vector is symmetrical distribution for any anisotropic materials. Especially, the direction of the refraction wave vector is coincident with that of the Poynting vector when $\theta_i = 0°$ and $\varphi = 0°$. After further studying, we find that when the incident angle θ_i and the metallic tilted angle φ satisfy the relationship as follows:

$$\theta_i(\varphi) = \pm \sin^{-1}\sqrt{\frac{2\alpha\left[\sqrt{1 + \frac{(\eta^2 - 4\alpha\beta)\eta^2}{4\alpha^2((\alpha-\beta)^2 + \eta^2)}} - 1\right]}{(\eta^2 - 4\alpha\beta)\varepsilon_r\mu_r}} \quad (22)$$

$\theta_s = \theta_t$, meaning their directions of the refraction wave vector and the Poynting vector are coincident. In the case of $\varepsilon_x > 0$ and $\varepsilon_z > 0$ with $\varphi < 0$ in Fig. 3c, it is not hard to find that when $\theta_i < 0$, $\theta_s = \theta_t$. In the case of $\varepsilon_x > 0$ and $\varepsilon_z < 0$ with $\varphi < 0$ in Fig. 3f; however, it is obvious that when $\theta_i > 0$, $\theta_s = \theta_t$.

Exotic Properties in Nonlinear Response

In Figs. 4 and 5, we plot the transmissivity t and the energy-flow angle θ_s as a function of the normalized intensity of external electric field E_0^2/E_c^2 for different incident angles θ_i, and their isofrequency dispersion curves in the metamaterials of Kerr-type nonlinearity with $\varphi = -45°$. Figures 4 and 5 correspond to the self-focusing nonlinearity ($\zeta = 1$) and self-defocusing nonlinearity ($\zeta = -1$), respectively. From Figs. 4 and 5, we can see that the propagation properties of waves/light, including their propagation direction and transmissivity, can be controlled by the external electric field. In Fig. 4a, b, we find that for a fixed incident angle $\theta_i = 0°$ or 30° (in general, when $0 \le \theta_i < \theta_{c1}(\varphi)$), the TM-polarized light transmission in the composite structure is cut-off when $E_0 = 0$ or E_0^2/E_c^2 less than a certain value (about 1.6). However, if the external field intensity is increased to $2 < E_0^2/E_c^2 < 6$, the TM-polarized light break-overs and has very high transmissivity, and the energy flow is negative refraction ($\theta_s < 0$), as shown in Fig. 4e, f. However, for a fixed incident angle

$\theta = 45°$ or 60° (in general, when $\theta_{c1}(\varphi) < \theta_i < 90°$), as shown in Fig. 4c, d, some different features occur compared with Fig. 4a, b. To be specific, when $E_0 = 0$ or E_0^2/E_c^2 is greater than the critical value (about 1.6), there are high transmittance and what's more different is that the energy-flow angle has different sign for $E_0 = 0$ and $E_0^2/E_c^2 > 1.6$, as shown in Fig. 4g, h, which means that the energy-flow angle (i.e., the direction of the energy flow) is tunable by controlling the intensity of the external electric field. In other words, we can realize the dynamic transformation of energy flow from positive refraction to cut-off and then to negative refraction by regulating the intensity of the applied electric field.

It is well known that the energy-flow direction is coincident with the direction of the group velocity for plane waves, $\mathbf{V}_g = \nabla_\mathbf{K}\omega(\mathbf{K})$. They are not necessarily parallel to the wave vector in anisotropic materials. $\nabla_\mathbf{K}\omega(\mathbf{K})$ must lie normal to the isofrequency contour, $\omega(\mathbf{K}) = const$. The general relationship between the directions of energy flow and refraction wave vector for waves propagating in the metamaterial can also be demonstrated by the isofrequency dispersion contour, as illustrated in Fig. 4i, j, and they show a good agreement with the other figures in Fig. 4. From Fig. 4i, we can see that in the limit of $E_0^2/E_c^2 = 0$, when the incident angle is less than a certain critical angle, there exists no refraction wave vector; consequently, there is no energy-flow transmission in the metamaterial, due to the phase mismatching between the refraction wave vector and incident wave vector at the boundary interface. When the incident angle is larger than the critical angle $\theta_{c1}(\varphi)$, however, there exists refraction wave vector; consequently, there is energy-flow transmission into the metamaterial, and both the refraction wave vector and energy flow are positive refraction, as illustrated in Fig. 4i, which is coincident with the energy flow shown in Fig. 4g, h. From Fig. 4j, we can see that when $E_0^2/E_c^2 = 4$, there exists refraction wave vector, as well as energy-flow transmission into the metamaterial; what's more, the refraction wave vector is positive refraction, while the energy flow is negative refraction.

Similarly, there exist some analogous properties in the case of self-defocusing nonlinearity ($\zeta = -1$), shown in Fig. 5. When the intensity of the applied electric field is smaller than a certain value ($0 \le E_0^2/E_c^2 < 2$), that the energy-flow angle is negative and belongs to negative refraction; when it is increased to $2 < E_0^2/E_c^2 < 4 - \sin^2(\theta_i)$, the energy flow is switched off and there is no refraction wave, as shown in the yellow area. Then increasing further the intensity of the applied electric field, the energy flow is switched on again, and its refraction angle becomes positive, belonging to positive refraction. Therefore, it is also possible that the dynamic transformation of energy flow from negative refraction to cut-off and then to positive refraction by regulating the
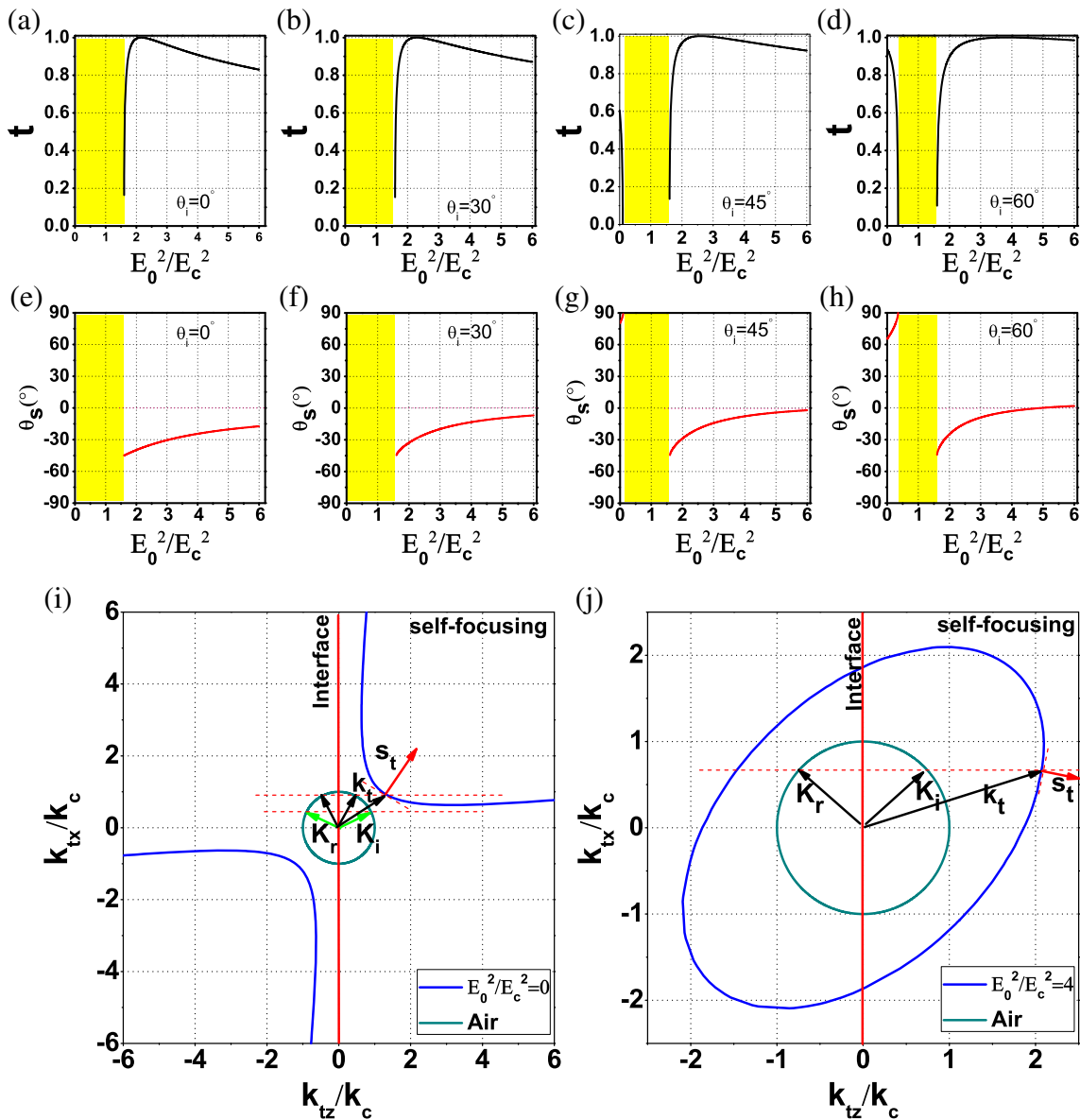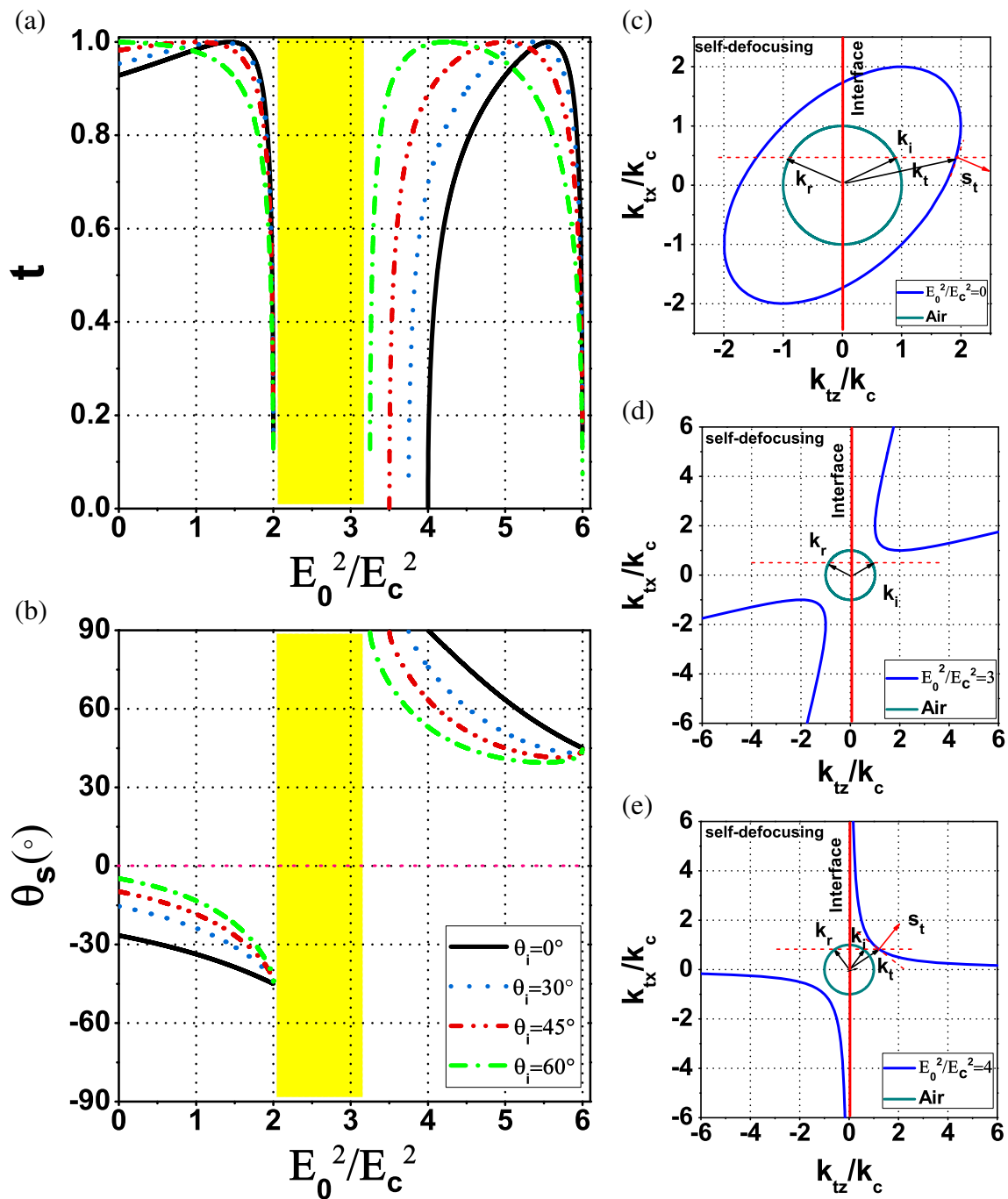
Fig. 4 The transmissivity t, the energy-flow angle θ_s, and the isofrequency dispersion curves versus the normalized intensity of external electric field E_0^2/E_c^2 in the case of self-focusing nonlinearity, with $\varphi = -45°$, $\zeta = 1$, $\epsilon_{D0} = 2.4$, $k_c = \omega/c$. **a**–**d** and **e**–**h** correspond to the transmissivity and energy flow angle for four different incident angles $\theta_i = 0°, 30°, 45°, 60°$, respectively. **i** and **f** are the isofrequency dispersion curves for self-focusing case in the condition

of $E_0^2/E_c^2 = 0$ and $E_0^2/E_c^2 = 4$, respectively, where dark cyan and blue lines denote the dispersion curves in air and the nonlinear metamaterial, respectively. $\mathbf{K}_i$, $\mathbf{K}_r$, $\mathbf{K}_t$ and $\mathbf{S}_t$ represent incident wave vector, reflection wave vector, refraction wave vector and energy-flow vector, respectively. Red dashed lines denote the continuity of tangential wave vector

applied electric field in the metamaterial of self-defocusing nonlinearity. These properties can be demonstrated through the isofrequency dispersion curves, as illustrated in Fig. 5c–e. From Fig. 5c, we can see that when $E_0^2/E_c^2 = 0$, there exists always refraction wave vector; consequently, there is energy-flow transmission into the metamaterial, and the energy flow are negative refraction, as shown by the red arrow. But when $E_0^2/E_c^2 = 3$, as shown in Fig. 5d,

there exists not any refraction wave; consequently, there is no energy-flow transmission into the metamaterial. When $E_0^2/E_c^2 = 4$, there exist refraction wave vector and energy-flow transmission into the metamaterial again, and the energy flow are positive refraction. These properties make it possible for nonlinear metamaterials to be widely used in all-optical switching, all-optical routing, and other nanophotonic devices. For the above analysis about Figs. 4

Fig. 5 The transmissivity t, the energy-flow angle θ_s, and the isofrequency dispersion curves versus the normalized intensity of external electric field E_0^2/E_c^2 in the case of self-defocusing nonlinearity, with $\varphi = -45°$, $\zeta = -1$, $\epsilon_{D0} = 6$, and $k_c = \omega/c$. **a** and **b** correspond the transmissivity and energy-flow angle for four different incident angles $\theta_i = 0°, 30°, 45°, 60°$ respectively. **c**, **d**, and **e** are the dispersion curves for self-defocusing case in the condition of $E_0^2/E_c^2 = 0$, $E_0^2/E_c^2 = 3$ and $E_0^2/E_c^2 = 4$, respectively, where dark cyan and blue lines, $\mathbf{K}_i$, $\mathbf{K}_r$, $\mathbf{K}_t$, and $\mathbf{S}_t$ represent the same meaning as Fig. 4

and 5, we can know that there exists all-angle total reflection region (the yellow area), meaning that there is no energy transmission into the metamaterial for any incident angles, which is dependent on the orientation angle φ and the applied electric field E_0. To illustrate the

dependencies between them, the all-angle total reflection region (the area enclosed by the red lines) is shown in Fig. 6a, b for the self-focusing and self-defocusing cases, respectively. For instance, when $\varphi = -45°$, if all-angle total reflection phenomena occur, the required external

Fig. 6 The all-angle total reflection region enclosed by the red lines for different intensity of external electric field E_0^2/E_c^2 and the tilted angle φ for two cases. **a** $\zeta = 1$ (for self-focusing nonlinearity), $\epsilon_{D0} = 2.4$. **b** $\zeta = -1$ (for self-defocusing nonlinearity), $\epsilon_{D0} = 6$. The yellow area corresponds to the total reflection region when $\varphi = -45°$
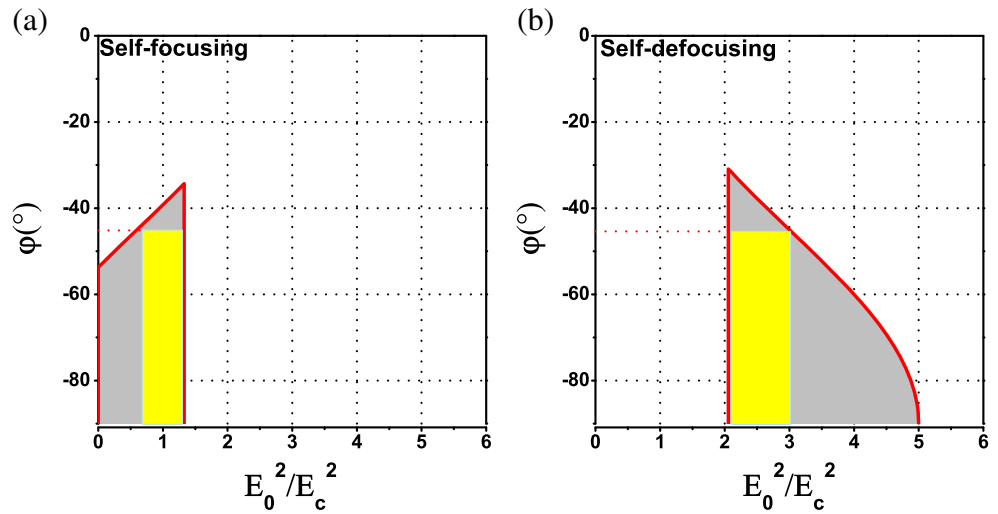
electric field is $0.6 < E_0^2/E_c^2 < 1.33$ (yellow area) for self-focusing nonlinearity, and $2 < E_0^2/E_c^2 < 3$ (yellow area) for self-defocusing nonlinearity, which are consistent with those in Figs. 4 and 5, respectively. The property of all-angle total reflection has wide potential applications in optoelectronic fields such as wave cut-off devices.

In addition, from Figs. 4 and 5, we can see that the transmissivity can equal to 1 in the limit of lossless. When the total transmission phenomenon occur, at this point, the incident angle is called the Brewster angle. In Eq. 19, if $t = 1$, the Brewster angle can be obtained as follows:

$$\theta_b = \sin^{-1} \frac{2\sqrt{\mu_r - \varepsilon_r \mu_y^2 \alpha}}{\sqrt{(\eta^2 - 4\alpha\beta)\mu_r \varepsilon_r^2 \mu_y^2 + 4\mu_r}} \quad (23)$$

Figure 7 shows the changes of Brewster angle with the intensity of the external electric field for self-defocusing and self-focusing cases with $\varphi = 0°, -30°, -45°,$ and $-60°,$

respectively. From Fig. 7 and Eq. 23, it is not hard to see that the mutual dependency relation between applied electric field intensity and incident angle when total transmission phenomenon occurs for different orientation angles φ. This is helpful for us to analyze and design all-optical switches and routers. It is worth noting that the materials used in the metamaterial are not specified, but we can find some materials of the strong focusing nonlinearity such as $n - InSb$, and those of the strong defocusing properties such as $Ba_x Sr_{1-x} TiO3$ [7].

All-Optical Switching and Routing Optimal Designs

From the above features, we can see that this kind of non-linear metamaterials would have widely potential application in the field of nanophotonic functional materials and devices. In order to optimize their characteristics, facilitating device design and application, Table 1 shows light states, the transmissivity t, the energy-flow refraction angle θ_s, the

Fig. 7 Brewster angle versus the intensity of external electric field E_0^2/E_c^2 for $\varphi = 0°, -30°, -45°, -60°$ in two cases. **a** $\zeta = -1$ (for self-defocusing nonlinearity), $\epsilon_{D0} = 6$. **b** $\zeta = 1$ (for self-focusing nonlinearity), $\epsilon_{D0} = 2.4$
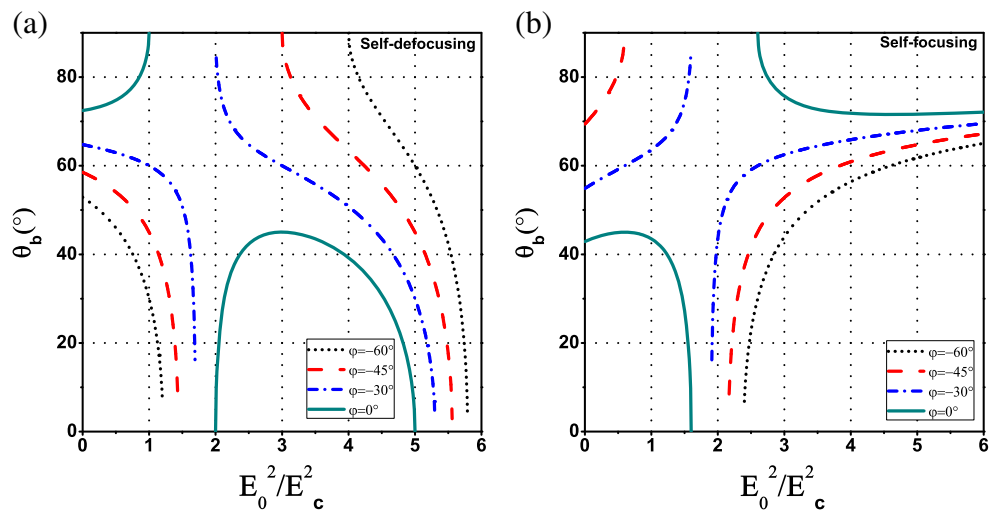
Table 1 Light states, the transmissivity t, the energy-flow refraction angle θ_s, the needed intensity of external electric field E_0^2/E_c^2 and φ in the case of normal incidence to the interface between air and the metamaterial for self-defocusing and self-focusing nonlinearity, respectively

Nonlinear styles	$\theta_i(°)$	$\varphi(°)$	E_0^2/E_c^2	$\theta_s(°)$	t	Light states
Self-defocusing	0	− 45	1.44	− 38.0	1	Negative refraction
			[2, 4]	/	0	Cut-off
			5.56	52.0	1	Positive refraction
		− 90	1	0	1	Normal refraction
			[2, 6]	/	0	Cut-off
Self-focusing	0	− 20	1.75	− 64.4	1	Negative refraction
			[1.13, 1.60]	/	0	Cut-off
			0	48.6	0.91	Positive refraction
		− 90	2.6	0	1	Normal refraction
			[0, 1.60]	/	0	Cut-off

needed intensity of external electric field E_0^2/E_c^2, and φ in the case of normal incidence to the interface between air and the metamaterial for self-defocusing and self-focusing nonlinearity, respectively. From Table 1, we can see that, on the one hand, under the conditions of normal incidence and $\varphi = -90°$, when $E_0^2/E_c^2 = 1$ for self-defocusing nonlinearity or $E_0^2/E_c^2 = 2.6$ for self-focusing nonlinearity, light propagates perpendicular to the interface and without deflection ($\theta_s = 0$, called normal refraction states), and it is full transmission ($t = 1$). However, when $E_0^2/E_c^2 \in [2, 6]$ for self-defocusing nonlinearity or $E_0^2/E_c^2 \in [0, 1.60]$ for self-focusing nonlinearity, light does
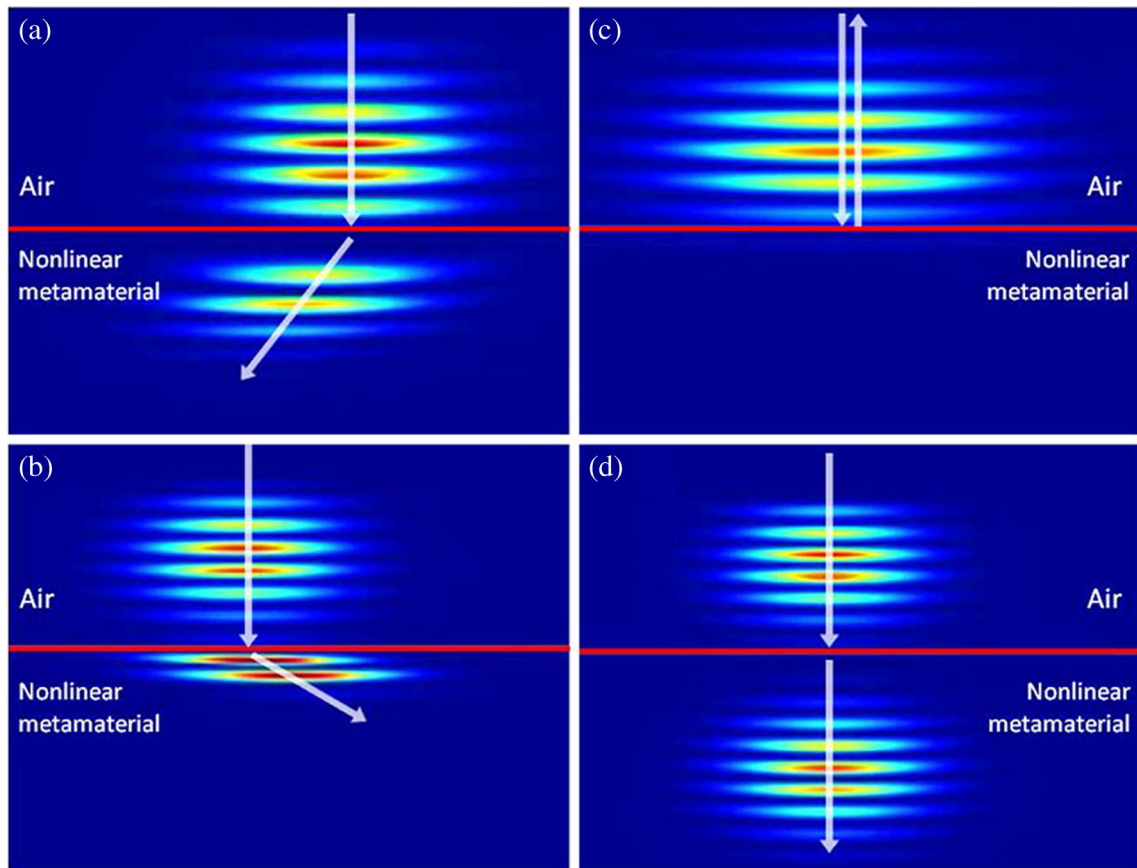
Fig. 8 The numerical simulations of a Gaussian wave propagation at an Air-Nonlinear metamaterials (Self-defocusing) interface. Arrows indicate the directions of motion. Red lines indicate the interface between air and self-defocusing nonlinear metamaterials. **a** Negative refraction state for $\varphi = -45°$, $E_0^2/E_c^2 = 1.44$. **b** Positive refraction state for $\varphi = -45°$, $E_0^2/E_c^2 = 5.56$. **c** Cut-off state for $\varphi = -90°$, $E_0^2/E_c^2 = 3$. **d** Normal refraction state for $\varphi = -90$, $E_0^2/E_c^2 = 1$

not transmit, and is reflected totally ($t = 0$), called cut-off states. These characteristics can be applied to all-optical switching design. On the other hand, under the conditions of normal incidence, by designing suitable orientation angles φ, the interconversion among positive refraction, negative refraction, and cut-off states is feasible by adjusting the intensity of the applied electric field. The simulation with Gaussian wave [38, 39] has been made to validate the correctness of the above theoretical calculations as shown in Fig. 8. For example, in Fig. 8a, b, when $\varphi = -45°$ and light propagates perpendicular to the interface for self-defocusing nonlinear metamaterials , we can adjust the refraction directions of light from negative ($\theta_s = -38.0°$) to positive ($\theta_s = 52.0°$) states by changing the normalized intensity of the applied electric field from 1.44 to 5.56. These characteristics can be applied to all-optical routing design. What's more, in Fig. 8c, d, when $\varphi = -90°$ and light propagates perpendicular to the interface for self-defocusing nonlinear metamaterials, we can change the light states from cut-off to normal refraction states ($\theta_s = 0°$) by adjusting the normalized intensity of the applied electric field from 3 to 1. It can be applied to all-optical switching design. In addition, there are similar characteristics for self-focusing nonlinear metamaterials.

Conclusions

We have investigated exotic propagation characteristics of TM-polarized light in the nonlinear metamaterials composed of conducting nanowire array embedded into a nonmagnetic host medium with a Kerr-type nonlinearity. We have demonstrated that controlling the propagation direction and propagation states (ON or OFF) of light is possible by adjusting the intensity of applied electric field. In addition, all-angle total reflection phenomena exist in such nonlinear metamaterials by choosing a suitable tilted angle of nanowires and the intensity of external electric field. These properties make this kind of nonlinear metamaterials have widely potential applications in all-optical switches, all-optical routers, wave cut-off devices, and other nanophotonic devices.

References

1. Burgos SP, De WR, Polman A, Atwater HA (2010) A single-layer wide-angle negative-index metamaterial at visible frequencies. Nat Mater 9(5):407–412
2. Hao J, Yuan Y, Ran L, Jiang T, Kong JA, Chan CT, Zhou L (2007) Manipulating electromagnetic wave polarizations by anisotropic metamaterials. Phys Rev Lett 99(6):063908
3. Ginzburg P, Rodríguez Fortuño FJ, Wurtz GA, Dickson W, Murphy A, Morgan F, Pollard RJ, Iorsh I, Atrashchenko A, Belov PA (2013) Manipulating polarization of light with ultrathin epsilon-near-zero metamaterials. Opt Express 21(12):14907–14917
4. Smson ZL, Macdonald KF, Angelis FD, Gholipour B, Knight K, Huang CC, Fabrizio ED, Hewak DW, Zheludev NI (2010) Metamaterial electro-optic switch of nanoscale thickness. Appl Phys Lett 96(14):551
5. Shoaei M, Moravvejfarshi MK, Yousefi L (2015) All-optical switching of nonlinear hyperbolic metamaterials in visible and near-infrared regions. J Opt Soc Am B 32(11):2355–2363
6. Li W, Liu Z, Zhang X, Jiang X (2012) Switchable hyperbolic metamaterials with magnetic control. Appl Phys Lett 100(16):3966
7. Zharov AA, Shadrivov IV, Kivshar YS (2003) Nonlinear properties of left-handed metamaterials. Phys Rev Lett 91(3):037401
8. Lapine M, Gorkunov M, Ringhofer KH (2003) Nonlinearity of a metamaterial arising from diode insertions into resonant conductive elements. Phys Rev E 67(2):065601
9. Poutrina E, Huang D, Smith DR (2010) Analysis of nonlinear electromagnetic metamaterials. New J Phys 12(9):093010
10. Yang R, Shadrivov IV (2010) Double-nonlinear metamaterials. Appl Phys Lett 97(23):231114
11. Lerosey G, De Rosny J, Tourin A, Fink M (2007) Focusing beyond the diffraction limit with far-field time reversal. Science 315(5815):1120–1122
12. Verslegers L, Catrysse PB, Yu Z, Fan S (2009) Deep-subwavelength focusing and steering of light in an aperiodic metallic waveguide array. Phys Rev Lett 103(3):033902
13. Silveirinha MG (2013) Theory of spatial optical solitons in metallic nanowire materials. Phys Rev B 87(23):235115
14. Dani KM, Ku Z, Upadhya PC, Prasankumar RP, Brueck S, Taylor AJ (2009) Subpicosecond optical switching with a negative index metamaterial. Nano Lett 9(10):3565–3569
15. Shadrivov IV, Morrison SK, Kivshar YS (2006) Tunable split-ring resonators for nonlinear negative-index metamaterials. Opt Express 14(20):9344–9349
16. Sun L, Li Z, Luk TS, Yang X, Gao J (2015) Nonlocal effective medium analysis in symmetric metal-dielectric multilayer metamaterials. Phys Rev B 91(19):195147
17. Geng T, Zhuang S, Gao J, Yang X (2015) Nonlocal effective medium approximation for metallic nanorod metamaterials. Phys Rev B 91(24):245128
18. Yao J, Liu Z, Liu Y, Wang Y, Sun C, Bartal G, Stacy AM, Zhang X (2008) Optical negative refraction in bulk metamaterials of nanowires. Science 321(5891):930–930
19. Kante B (2009) Metamaterials, from micro-wave to optics: theory and applications. Ann Phys 34(2-3):1–120
20. Pitarke J, Garcia-Vidal F, Pendry J (1998) Effective electronic response of a system of metallic cylinders. Phys Rev B 57(24):15261
21. Maslovski S, Tretyakov S, Belov P (2002) Wire media with negative effective permittivity: a quasi-static model. Microw Opt Technol Lett 35(1):47–51

22. Silveirinha MG, Belov PA, Simovski CR (2008) Ultimate limit of resolution of subwavelength imaging devices formed by metallic rods. Opt Lett 33(15):1726–1728
23. Belov PA, Hao Y, Sudhakaran S (2006) Subwavelength microwave imaging using an array of parallel conducting wires as a lens. Phys Rev B 73(3):033108
24. Silveirinha MG (2006) Additional boundary condition for the wire medium. IEEE Trans Antennas Propag 54(6):1766–1780
25. Belov PA, Simovski CR, Ikonen P (2005) Canalization of subwavelength images by electromagnetic crystals. Phys Rev B 71(19):193105
26. Ye F, Mihalache D, Hu B, Panoiu NC (2010) Subwavelength plasmonic lattice solitons in arrays of metallic nanowires. Phys Rev Lett 104(10):106802
27. Lemoult F, Fink M, Lerosey G (2011) Revisiting the wire medium: an ideal resonant metalens. Wave Random Complex 21(4):591–613
28. Belov PA, Silveirinha MG (2006) Resolution of subwavelength transmission devices formed by a wire medium. Phys Rev E 73(5):056607
29. Lai Y, Hui P (2013) Surface plasmon dispersion relation of a metallic wire in a nonlinear dielectric medium. Opt Commun 304:111–115
30. Wang Y, Plummer E, Kempa K (2011) Foundations of plasmonics. Adv Phys 60(5):799–898
31. Shvonski AJ, Kong J, Kempa K (2017) Nonlocal extensions of the electromagnetic response of plasmonic and metamaterial structures. Phys Rev B 95(4):045149
32. Shoaei M, Yousefi L, Moravvejfarshi MK (2015) Nanostructured graphene-based hyperbolic metamaterial performing as a wide-angle near infrared electro-optical switch. Appl Opt 54(5):1206–1211
33. Wang H, Wu J, Guo J, Jiang L, Xiang Y, Wen S (2016) Low-threshold optical bistability with multilayer graphene-covering Otto configuration. J Phys D Appl Phys 49(25):255306
34. Zhao HJ, Li ZH (2013) Low-threshold optical bistability in metal-nonlinear dielectric multilayer nanostructure. Epl 102(2):24003
35. Jian-Hua Z, Hai-Lu L, Shuang-Chun W, An-Le F, Bin-Xian Z (2009) Anomalous phenomena of electromagnetic wave propagation in metamaterials for arbitrary orientation of optical axis. Acta Phys Sin-Ch Ed 58(3):1765–1772
36. Smith D, Schurig D (2003) Electromagnetic wave propagation in media with indefinite permittivity and permeability tensors. Phys Rev Lett 90(7):077405
37. Zhao H, Zhang J, Wang G (2017) Engineering hybrid guided modes in subwavelength uniaxial metamaterial waveguides. Plasmonics 12(2):245–255
38. Lu W, Sokoloff J, Sridhar S (2004) Refraction of electromagnetic energy for wave packets incident on a negative-index medium is always negative. Phys Rev E 69(2):026604
39. Smith D, Schurig D, Pendry J (2002) Negative refraction of modulated electromagnetic waves. Appl Phys Lett 81(15):2713–2715